Improving the extreme temperature measurement capability of FBG sensors encapsulated in low thermal expansion materials

Gerard Natividad [1], Julian McIntyre [1], Suzana Turk [1], Daniel Bitton [1], Alison Lockley [2], Trent Schultz [2], David Hartley [2] and Chris Wood [2]

[1] *Defence Science and Technology Group, 506 Lorimer Street, Fishermans Bend 3207, Victoria, Australia*
[2] *Defence Science and Technology Group, Eagle Farm QLD 4009*

Abstract

Fibre Bragg grating (FBG) sensors are an attractive sensing solution for temperature and strain measurements where immunity to electromagnetic interference, high spatial resolution, and low spatial intrusiveness is required. The temperature sensing capability of FBG sensors is based on the wavelength response induced by the thermo-optic coefficient of the silica glass core and, to a lesser extent, its coefficient of thermal expansion (CTE). Since the CTE contribution to wavelength response in moderate temperature ranges (< 200°C) is small, this factor is normally neglected [1]. However, the exclusion of CTE may lead to significant measurement errors at elevated temperatures, such as in the thermal performance assessment of materials and components used in thermal protection systems. Therefore, the CTE contribution to wavelength response must be included when measuring through-thickness temperature in low CTE ablative materials exposed to high heat fluxes.

The effect of a low thermal expansion material on the temperature sensitivity of FBG sensors subjected to temperatures up to 300°C was investigated in the current work. By characterising and accounting for the influence of CTE on the wavelength response of FBG sensors encapsulated in low CTE materials, the calibration equation obtained in this study will enable accurate temperature measurements at extreme temperatures.

Keywords: coefficient of thermal expansion, extreme temperature measurement, fibre Bragg gratings.

Introduction

Accurate thermal performance assessment of thermal protection systems (TPS) materials is an important part of the development and advancement of high-speed, long-range platforms. For example, thermal conductivity is a key qualifying factor used in the assessment of ablative materials for the development of TPS. This process relies on empirical measurements of both the surface and through-thickness temperature of the material which is normally achieved using optical pyrometers and thermocouples inserted in blind-holes at various depths [2]. These methods provide a limited number of temperature measurements which may lead to inaccurate characterisation of the material's internal temperature response to high heat fluxes during thermal loading. Embedment of quasi-distributed FBG sensors in every layer of a composite ablative material enables accurate thermal performance characterisation of the TPS without affecting the integrity of the material or component.

To determine the suitability of FBG sensors for this application, temperature calibration experiments were conducted on type II FBG sensors encapsulated in a low thermal expansion material matrix. The resulting calibration equations were then comparatively evaluated and applied to an embedded FBG sensor for internal temperature measurement of a low CTE C-C

composite coupon undergoing thermal loading. This study aims to improve the temperature measurement accuracy of FBG sensors embedded in low CTE materials for future ablative tests.

Experimental Method

Type II FBGs were fabricated using the femtosecond laser point-by-point inscription method at the Macquarie University ANFF OptoFab facility [3]. These sensors have an operational temperature range up to 800°C without exhibiting wavelength drift [4]. Temperature calibration experiments were conducted on two FBG sensors under different thermal expansion conditions, which are outlined in Table 1.

Table 1: Thermal expansion conditions for each temperature calibration experiment

Experiment	FBG	Description
Experiment 1: Unconstrained FBG	FBG1	The FBG sensor was bonded to one end of a copper capillary tube to allow unconstrained/natural thermal expansion during thermal loading
Experiment 2: Axially constrained FBG	FBG1	The FBG sensor was bonded to both ends of the copper capillary tube which was then axially constrained using the Instron universal testing system to prevent thermal expansion during thermal loading
Experiment 3: Embedded FBG	FBG2	The FBG sensor was embedded between the plies of a near-zero CTE C-C composite coupon during thermal loading

In experiments 1 and 2, a copper capillary tube was used to encapsulate FBG1 and was subjected to a stepped thermal profile up to 250°C. Each of these experiments were conducted three times and the calibration equations were calculated based on the combined datasets from each experiment. For Experiment 2, additional components (Figure 1) were used for both mechanical protection and bonding of the FBG sensor at the egress points of the copper tube. The entire assembly was then placed between platens installed on the Instron universal testing system which was held in zero displacement control during thermal loading to prevent thermal expansion of the copper tube and FBG sensor. In Experiment 3, the C-C composite coupon (Figure 2) was subjected to a ramped thermal profile reaching approximately 200°C using a high-intensity infrared test system (HIIRTS).

In each experiment, the wavelength response of the FBG sensor was recorded using the HYPERION si255 optical interrogator (± 1 pm wavelength accuracy) and compared with temperature measurements obtained using a co-located K-type micro-thermocouple. Calibration equations and temperature sensitivity values were derived from Experiments 1 – 3 and applied to another type II FBG sensor embedded in an additional C-C composite coupon as outlined in Experiment 3 for internal temperature measurement. A co-located K-type micro-thermocouple was used for experimental validation of these measurements.

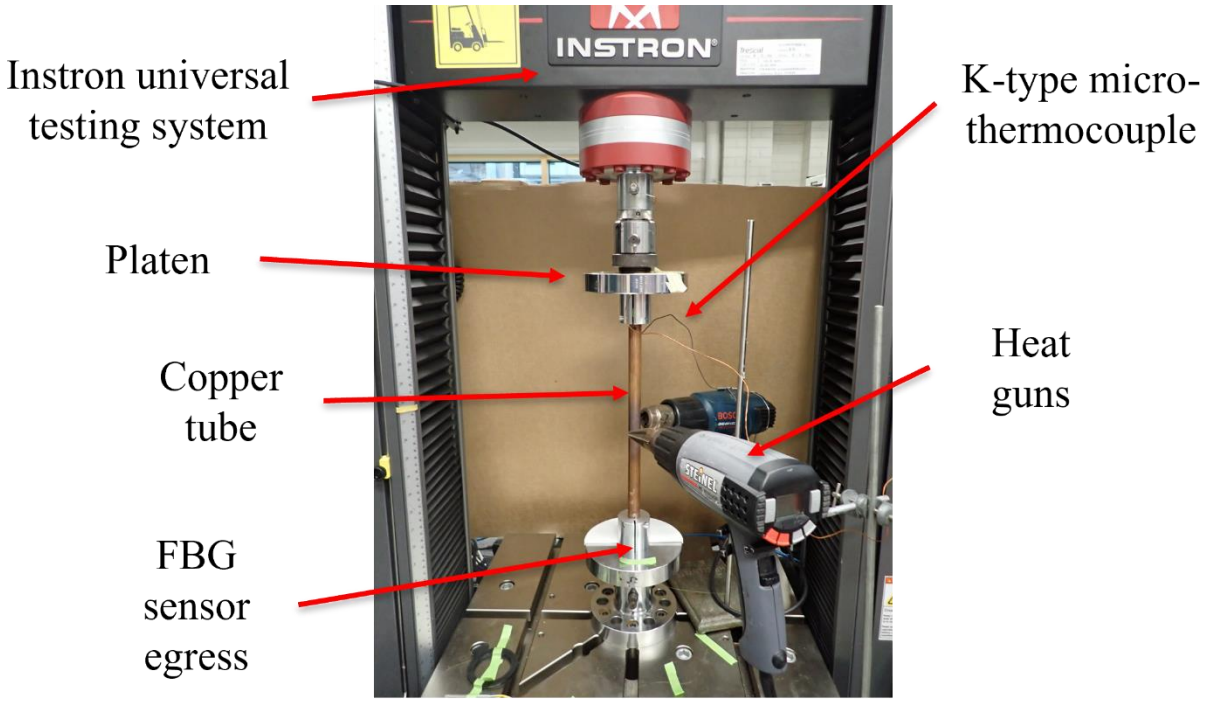

Figure 1: Encapsulation method used for axially constrained FBG (Experiment 2)

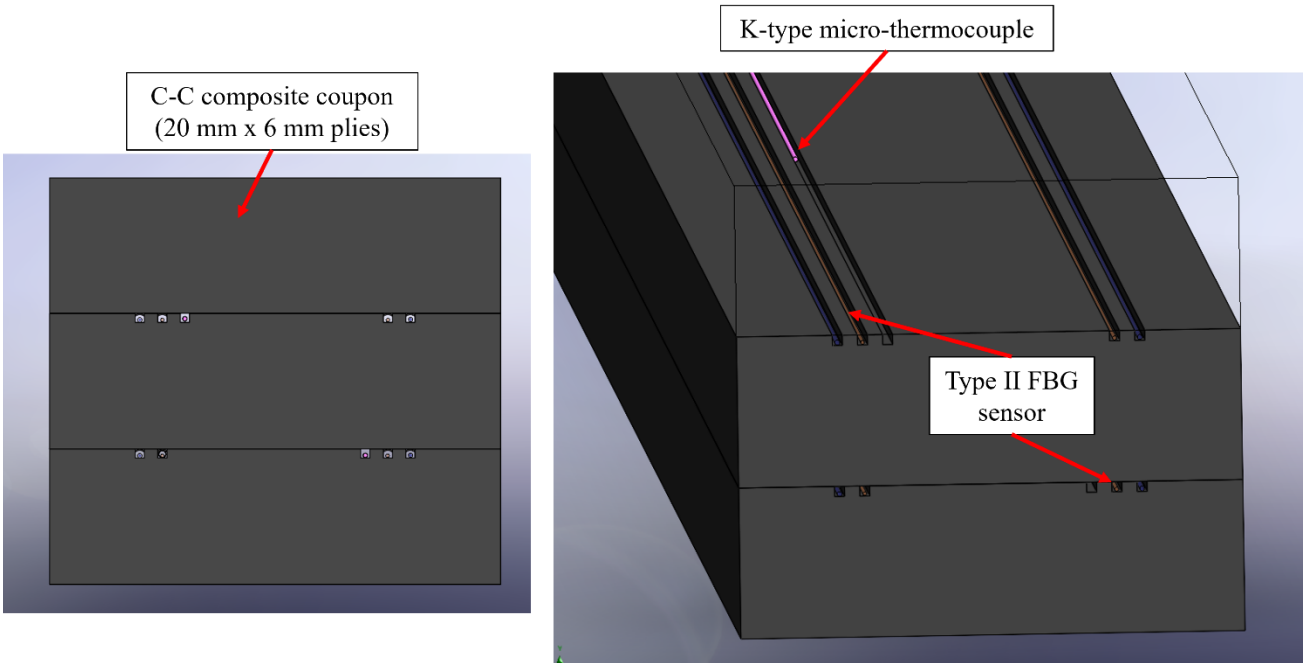

Figure 2: C-C coupon FBG sensor installation layout

Results

Figure 3 shows the wavelength response of each FBG sensor subjected to different thermal expansion conditions outlined in Table 1. For each experiment, linear regression was performed to derive the temperature calibration equations, which are represented by the dashed lines. All equations yielded a linear correlation of determination value greater than 0.99 which indicates a strong linear relationship between temperature and FBG wavelength response within this temperature range. The calibration equations, temperature sensitivities, and R^2 values are shown in Table 2. Note that Experiments 1 and 2 were conducted three times, with the FBG being allowed to cool to room temperature between each test.

Table 2: Calibration equations and temperature sensitivity values obtained from each experiment

Experiment	**R^2**	**Calibration equation**	**Temperature sensitivity** (pm/°C)
1 (*Unconstrained*)	0.99245	$\Delta\lambda = 0.01210 \cdot T - 0.326$	12.10
2 (*Axially constrained*)	0.99428	$\Delta\lambda = 0.01336 \cdot T - 0.413$	13.36
3 (*Embedded*)	0.99954	$\Delta\lambda = 0.01196 \cdot T - 0.3412$	11.96

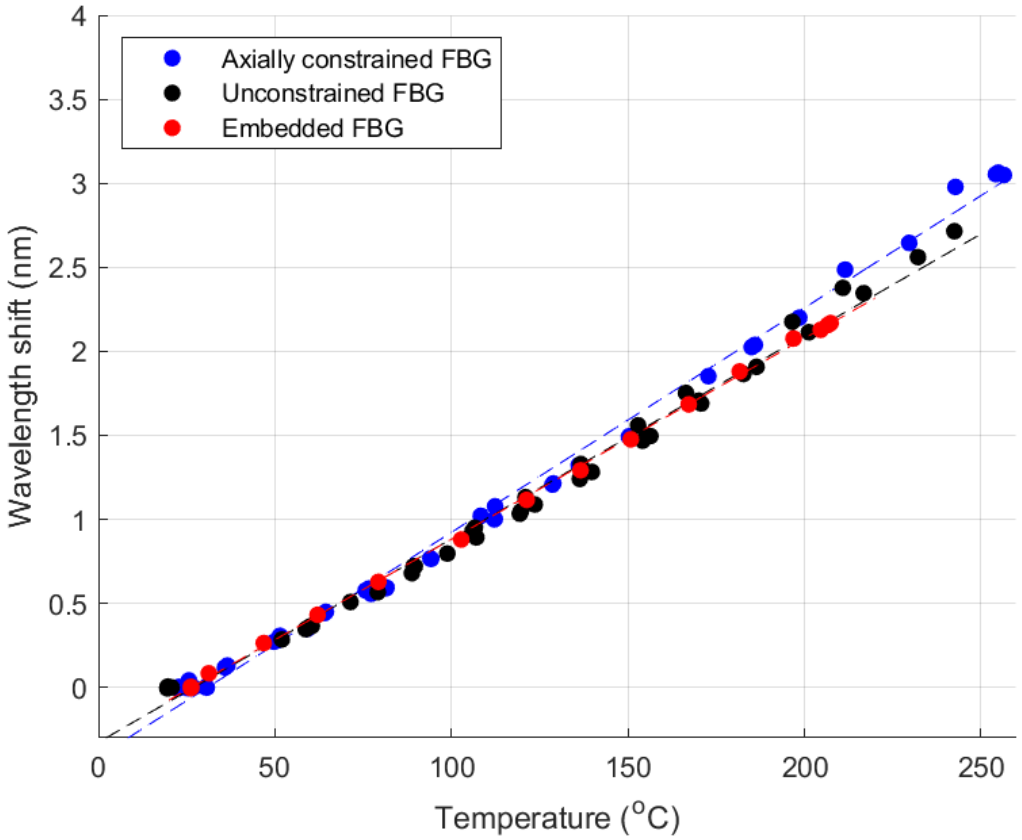

Figure 3: Wavelength response of type II FBGs under different thermal expansion conditions

The temperature sensitivity values obtained in Experiments 1 and 3 were consistent with each other and are within the ±1 pm wavelength accuracy of the optical interrogator. This is most likely due to the compatible CTE values of silica glass (0.55×10^{-6} /°C) and the C-C composite coupon (2.1×10^{-6} /°C). This result suggests that embedded FBG sensors can be used reliably for internal temperature measurement of materials with low CTE as the linear thermal expansion of the host material is similar to that of an unconstrained FBG sensor. However, this finding can only be applied to situations where the host material is allowed to freely expand and is not constrained by materials with significantly different CTE, such as steel motor casings (14.6×10^{-6} /°C) [5]. To further improve the temperature measurement capability of an embedded FBG sensor, a packaging technique to isolate the FBG from thermal strain induced by the host material was developed in this work.

Theoretically, preventing an FBG sensor from thermally expanding should yield a lower temperature sensitivity value compared to an unconstrained FBG as the contribution of CTE to the wavelength shift is removed. However, the temperature sensitivity value of the axially constrained FBG sensor (Experiment 2) was slightly higher than the values obtained in Experiments 1 and 3. This might be due to insufficient axial constraints which did not fully prevent thermal expansion of the copper capillary tube. It is also possible that the optical fibre

where the FBG is located was still able to expand thermally within the copper tube. Despite this, the temperature sensitivity value of the axially constrained FBG is still within the measurement error range of the optical interrogator.

To supplement these experiments, another C-C composite coupon was instrumented with type II FBG sensors and a co-located K-type micro-thermocouple. This coupon was exposed to the same intense radiative heat flux to a temperature of approximately 200°C using the HIIRTS. The wavelength response of the FBG was measured during thermal exposure and each of the temperature calibration equations shown in Table 2 were applied to obtain FBG temperature measurements. The results are shown in Figure 3 with thermocouple temperature measurements for experimental validation.

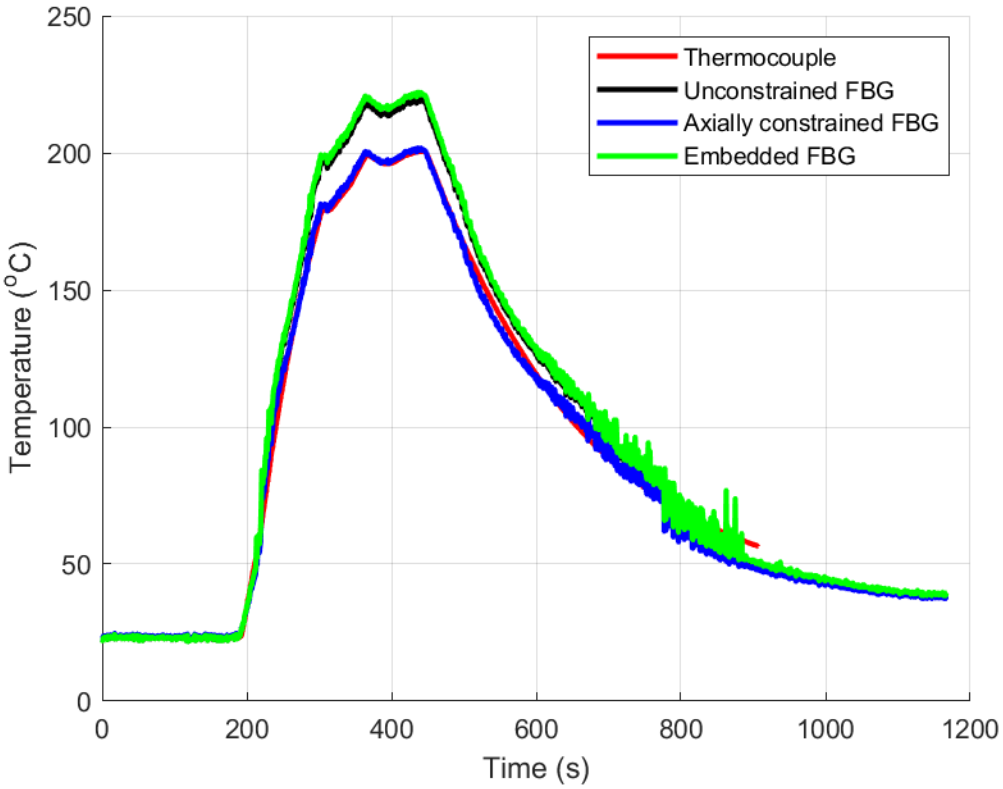

Figure 3: Internal temperature measurements of a C-C coupon using an embedded thermocouple and type II FBG sensor. The FBG temperature measurements were obtained by applying the calibration equations derived from Experiments 1 – 3.

The results show excellent correlation between the internal temperature measured by the type II FBG and the co-located thermocouple. The temperature measurements obtained using the unconstrained (Experiment 1) and embedded FBG calibration equations (Experiment 3) were in excellent agreement, which aligns with their similar temperature sensitivity values. However, these temperature measurements over-estimated the thermocouple temperature by approximately 20°C at 400 seconds exposure time. Application of the constrained calibration equation (Experiment 2) yielded the most accurate temperature measurements relative to the thermocouple temperature data due to the higher temperature sensitivity obtained in Experiment 2. However, this finding may be coincidental to the limitations in the experimental set-up used in Experiment 2. Overall, these results demonstrate the accuracy of FBG temperature measurements as validated by the thermocouple temperature data. However, more testing needs to be conducted to assess the reliability of FBG sensors embedded in low CTE ablative materials over a wider temperature range.

Conclusion

It was demonstrated that embedded type II FBG sensors can be used for accurate internal temperature measurement in low CTE materials. This was shown through the excellent agreement between the thermocouple and embedded FBG sensor temperature measurements. This finding can be used to improve the sensor installation strategies for use in thermal performance assessment of TPS materials and provide significantly more temperature data than conventional temperature sensors such as thermocouples. To further improve the temperature measurement accuracy of embedded FBG sensors, a new embedment packaging technique to isolate the FBG from thermal strain induced by the host material was successfully demonstrated. Preliminary results showed successful reduction of strain transfer from the host material, yielding improved temperature only measurements. Further work will be conducted to improve the robustness of this packaging technique and demonstrate its effectiveness in the thermal assessment of various aerospace components subjected to extreme thermal loading conditions.

Acknowledgements

The authors acknowledge Robert Zouev and David Russell from the Defence Science and Technology Group Fatigue and Fracture Laboratory (FFL) for their contributions to the temperature calibration experiments conducted using the Instron universal testing system.

References

1. G. F. Pereira, M. McGugan and L. P. Mikkelsen, “Method for independent strain and temperature measurement in polymeric tensile test specimen using embedded FBG sensors,” *Polymer Testing*, pp. 125-134, 2016, doi: https://doi.org/10.1016/j.polymertesting.2016.01.005.

2. H. T. Martin, “Assessment of the performance of ablative insulators under realistic solid rocket motor operating conditions,” Pennsylvania State University, 2013. [Online]. Available: https://ntrs.nasa.gov/api/citations/20130013898/downloads/20130013898.pdf

3. Australian National Fabrication Facility. “ANFF OptoFab”. anff.org.au. [Online.] Available: https://anff.org.au/locations/optofab-node/

4. S. J. Mihailov, D. Grobnic, C. Hnatovsky, R. B. Walker, P. Lu, D. Coulas and H. Ding, “Extreme environment sensing using femtosecond laser-inscribed fibre Bragg gratings,” *Sensors*, vol. 17, no. 12, 2017, doi: https://doi.org/10.3390/s17122909.

5. Matweb. “AISI 4140 Steel, normalized at 870°C (1600°F), reheated to 845°C (1550°F), oil quenched, 260°C (500°F) temper, 25 mm (1 in.) round”. Matweb.com. [Online.] Available: https://www.matweb.com/search/datasheet_print.aspx?matguid=27999b18ea6843d086b018e075821724